Estuaries and Coasts (2019) 42:112–131
https://doi.org/10.1007/s12237-018-0444-1

A Bayesian Approach to Predict Sub-Annual Beach Change and Recovery

Kat Wilson[1] · Erika E. Lentz[2] · Jennifer L. Miselis[3] · Ilgar Safak[2] · Owen T. Brenner[3]

Received: 10 January 2018 / Revised: 25 June 2018 / Accepted: 27 July 2018 / Published online: 27 August 2018

Abstract

The upper beach, between the astronomical high tide and the dune-toe, supports habitat and recreation along many beaches, making predictions of upper beach change valuable to coastal managers and the public. We developed and tested a Bayesian network (BN) to predict the cross-shore position of an upper beach elevation contour (Z_lD) following 1 month to 1-year intervals at Fire Island, New York. We combine hydrodynamic data with series of island-wide topographic data and spatially limited cross-shore profiles. First, we predicted beach configuration of Z_lD positions at high spatial resolution (50 m) over intervals spanning 2005–2014. Compared to untrained model predictions, in which all six outcomes are equally likely (prior likelihood = 0.16), our prediction metrics (skill = 0.52; log likelihood ratio = 0.14; accuracy = 0.56) indicate the BN confidently predicts upper beach dynamics. Next, the BN forecasted three intervals of beach recovery following Hurricane Sandy. Results suggest the pre-Sandy training data is sufficiently robust to require only periodic updates to beach slope observations to maintain confidence for forecasts. Finally, we varied input data, using observations collected at a range of temporal (1–12 months) and spatial (50 m to > 1 km) resolutions to evaluate model skill. This experiment shows that data collection techniques with different spatial and temporal frequencies can be used to inform a single modeling framework and can provide insight to BN training requirements. Overall, results indicate that BNs and inputs can be developed for broad coastal change assessment or tailored to a set of predictive requirements, making this methodology applicable to a variety of coastal prediction scenarios.

Keywords Bayesian network · Coastal geomorphology · Barrier island · Hurricane Sandy · Beach recovery

Introduction

Sandy coasts, including mainland beaches and barrier islands, are dynamic landforms on which morphologic evolution occurs over a variety of temporal and spatial scales. Change in these environments is controlled by a combination of factors including antecedent geology (Belknap and Kraft 1985; Riggs et al. 1995; Schwab et al. 2000), oceanographic conditions (e.g., Wright and Short 1984), sediment supply (Carter et al. 1987; Yang et al. 2005; Hapke et al. 2010), storm frequency and impacts (Morton and Sallenger 2003), sea level rise (Fitzgerald et al. 2008; Lorenzo-Trueba and Ashton 2014), and human intervention and infrastructure (ASBPA National Beach Nourishment Database 2017; Program for the Study of Developed Shorelines and references therein 2017), all of which can evolve independently alongshore and through time. Understanding and anticipating the evolution of dynamic coastal systems is critical in order to manage natural resources, and maintain existing and future communities and infrastructure (U.S. Climate Change Science Program 2009; Melillo et al. 2014). To identify, monitor, and model current and future areas of persistent vulnerability and prepare for short-term (storms, seasons to sub-annual) change, spatially and temporally comprehensive beach and dune morphologic observations are necessary.

Ideally, long-term (i.e., decades) coastal change observations with sub-seasonal site-specific frequency are collected at a study site. A long, high temporal resolution record provides detailed understanding of short-term morphologic behavior,

Communicated by David Reide Corbett

Electronic supplementary material The online version of this article (https://doi.org/10.1007/s12237-018-0444-1) contains supplementary material, which is available to authorized users.

✉ Kat Wilson
kathleen.wilson@utexas.edu

[1] Cherokee Nation Technologies contracted to U.S. Geological Survey, St. Petersburg Coastal and Marine Science Center, 600 4th St South, St Petersburg, FL 33701, USA

[2] U.S. Geological Survey, Woods Hole Coastal and Marine Science Center, 384 Woods Hole Rd, Woods Hole, MA 02543, USA

[3] U.S. Geological Survey, St. Petersburg Coastal and Marine Science Center, 600 4th St South, St Petersburg, FL 33701, USA

which we define here as less than 1 year, in addition to long-term trends and the influence of storms. Sustained coastal monitoring programs (e.g., Duck, North Carolina (Field Research Facility Data Portal 2017) and Narrabeen, Australia (Turner et al. 2016)) are able to measure event-scale processes such as storm-induced coastal change as well as monitor beach and dune recovery, which is generally thought to occur over years to decades (Morton et al. 1994; Priestas and Fagherazzi 2010; Houser et al. 2015). Recovery trends can be interrupted by small magnitude storm events, seasonal fluctuations in morphology, and localized human intervention, thus return of material to beaches and dunes is spatially and temporally nonlinear (Lee et al. 1998; Houser et al. 2015). Therefore, consistent and repeat surveys comprising a multi-year research program are necessary to observe the range of individual storms to natural beach and dune accretion.

In addition to observational data, models that predict coastal morphologic change can fill important gaps in our understanding and better anticipate where beaches may be more vulnerable or resilient to change, but none is without tradeoffs. A variety of empirical models have been developed to predict shoreline change and evolution of the beach and barrier island profile (e.g., Wright et al. 1985) from daily (Splinter et al. 2017) to long-term (decades to millennia) dynamics (Lorenzo-Trueba and Ashton 2014). However, such formulations routinely simplify the complexity of the system and governing equations by assuming equilibrium shoreline position (Miller and Dean 2004; Yates et al. 2009; Splinter et al. 2014) or limiting the dimensions of sediment transport to cross shore (Lorenzo-Trueba and Ashton 2014) or alongshore fluxes (e.g., Pelnard-Considere 1956). Further, as noted by Reeve et al. (2016), empirical formulations "tend to be process or scenario specific," which can limit the transferability between sites or time scales. Alternatively, process-based models such as XBeach (Roelvink et al. 2009) can be tuned to successfully reproduce site-specific morphologic predictions during storms, but are often impractical to apply regionally or over months to years to predict accretion due to computational expense (Reeve et al. 2016).

Bayesian networks (BNs) have gained popularity as a computationally inexpensive predictive tool and an alternative to empirical and process-based models that can account for unknowns and quantify uncertainties within numerous fields of earth science, including coastal research (Hapke and Plant 2010; Plant and Holland 2011; Plant and Stockdon 2012; Lentz et al. 2016). BNs are statistical inference tools which can incorporate qualitative and quantitative observational data to predict the likelihood of an outcome, which is used to report prediction confidence. Probabilistic models in the form of BNs do not attempt to resolve discrete physical processes such as sediment transport and wave forces in coastal settings and therefore are able to increase model efficiency and reduce system complexity to a set of observable conditions. Newly acquired data can be routinely and efficiently incorporated into a BN (Palmsten et al. 2013), which is advantageous in dynamic environments such as barrier islands. These traits allow BNs to supplement the application of empirical and multi-dimensional process-based models for temporal and spatial scales over which fewer constraints are known for process controls.

Existing barrier island BNs predict coastal change resulting from temporal end-members: sea level rise (Gieder et al. 2014; Gutierrez et al. 2015; Plant et al. 2016) and storms (Plant and Stockdon 2012; Palmsten et al. 2014; Wilson et al. 2015). Sea level rise studies target first-order controls on coastal change which inform morphologic predictions on decadal to centennial time scales corresponding to global sea level rise projections. BNs designed to predict storm impacts emphasize pre-storm morphology and short-term hydrodynamic processes. However, neither application emphasizes monthly to inter-annual time scales, which can be critical to support short-term landscape and habitat management. Furthermore, past studies have demonstrated that BNs can be used to directly assimilate observations (Hapke and Plant 2010) and successfully reproduce observed changes that were used in model and training (i.e., hindcasting) (Gutierrez et al. 2011, 2015). In order to expand beyond hindcast studies toward prediction of future coastal change (i.e., forecasting), there is a need to evaluate BN ability to make predictions of coastal change at locations or over survey intervals not included in training but have observations available to validate predictions.

In our study, we designed three experiments that combine extensive observations of beach morphology within a BN to test if the available data have sampled sufficient spatial and temporal variability to predict upper beach change at Fire Island, New York on intervals with a maximum of 1 year. First, using a decades-long time series of topographic beach surveys, we predict upper beach change at high spatial resolution along the island, which includes small communities, state and county parks, and undeveloped wilderness. Next, we predict beach recovery at varying time intervals along Fire Island following Hurricane Sandy. Finally, we capitalize on a variety of data types and explore the ability of BNs to make predictions across a variety of spatial scales and survey intervals that range from 1 month to a year. In the third test, sub-sampling of morphologic input data and evaluation of predictive skill provides insight to the minimum data requirements of a BN to confidently predict upper beach change, which can be used to guide standards of practice for future coastal monitoring efforts. Furthermore, the resulting framework provides a reduced complexity model useful for decision-making applications.

Study Site

Fire Island (Fig. 1) is a 50-km-long barrier island seaward from the south shore of Long Island, New York. An

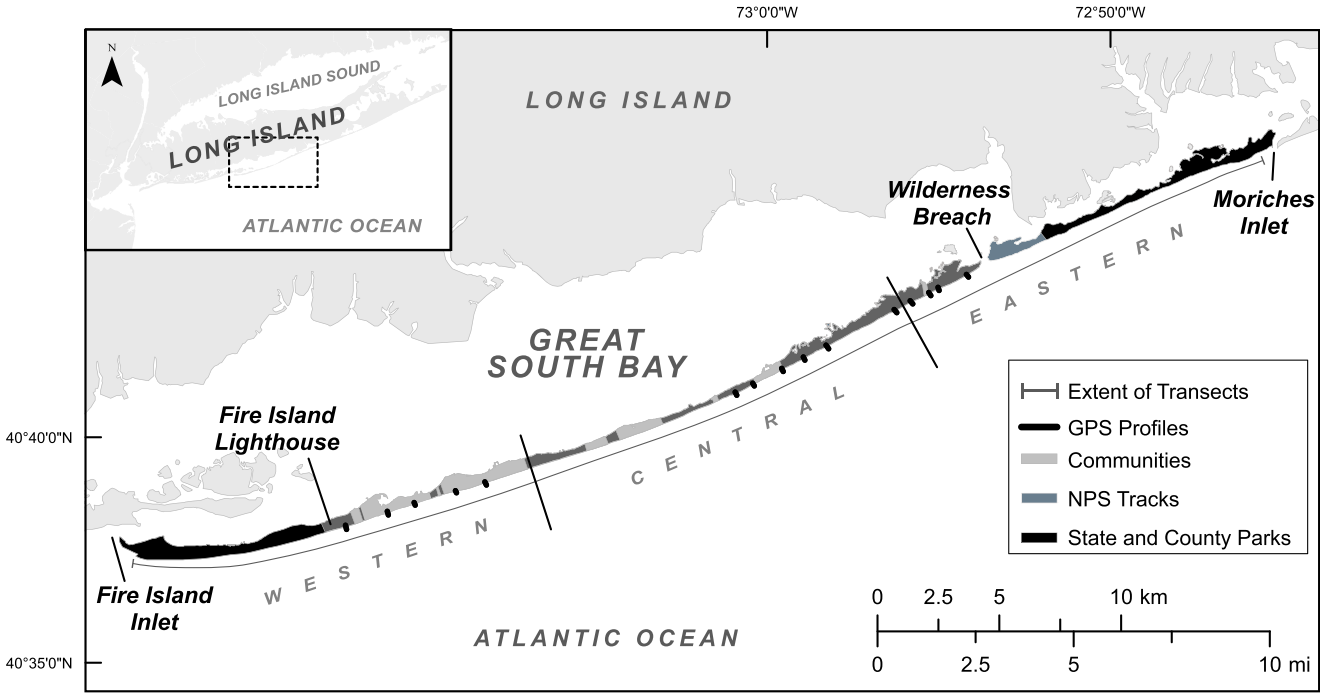

Fig. 1 Map of Fire Island, New York, showing the important state, county, and national park management zones and communities. Inset shows location of Fire Island in relation to Long Island and northeastern US coastline. The GPS profiles used to track post-Hurricane Sandy recovery are shown as black hashes. The alongshore coverage by 50-m spaced transects is indicated by the gray curve

established research program at Fire Island, New York has provided an understanding of local morphologic and hydrodynamic processes (Leatherman 1985; Lentz et al. 2013; Schwab et al. 2013; Schwab et al. 2014; Warner et al. 2014; Hapke et al. 2016) and a morphologic dataset (Table 1 in Supplemental Material) from which probabilistic models can be built and validated. Additionally, the severe impacts of Hurricane Sandy make Fire Island an ideal location to develop and test a BN to predict upper beach change, particularly related to recovery.

The majority of the island is within the Fire Island National Seashore and is managed by the National Park Service (NPS), although land use varies along the island. Within NPS-owned land, including the Otis Pike Fire Island High Dune Wilderness (herein: the Wilderness), development is limited to maintenance facilities, bayside marinas, and beach access walkways for visitors. On the east and west ends of the island respectively, Smith Point County Park and Robert Moses State Park maintain large, day-use facilities and infrastructure. Seventeen communities are interspersed within the national seashore and are comprised mainly of privately owned homes and businesses with few paved roads. Large-scale anthropogenic beach modification, including beach scraping (Bruun 1983; Kratzmann and Hapke 2012) and nourishment, on Fire Island has historically been focused within the communities, state and county parks, as described by Lentz et al. (2013). The island is bound by Fire Island Inlet in the west and Moriches Inlet in the east, and includes the Wilderness Breach, which formed during Hurricane Sandy in the eastern portion of the island and remains open as of December 2017.

The south shore of Long Island, including Fire Island, is affected by both extra-tropical and tropical storms, including five named storms since 2005 (Fig. 2) whose impacts have ranged from beach and dune erosion during the majority of storms to accretion in response to Hurricane Irene in 2011 (Brenner et al. 2018). In October 2012, Hurricane Sandy, the largest storm on record in the Atlantic basin (Blake et al. 2013; Safak et al. 2016; Warner et al. 2017), resulted in severe beach and dune erosion, widespread overwash, and multiple island breaches at Fire Island (Hapke et al. 2013). Hurricane Sandy was followed by several large, unnamed nor'easters and winter storms through the spring of 2013 (Hapke et al. 2013, 2016). The combined impacts of Hurricane Sandy and an unusually harsh winter resulted in an eroded beach state through April 2013 (Hapke et al. 2013; Brenner et al. 2018).

Immediately prior to Hurricane Sandy, the U.S. Geological Survey collected GPS data at ten locations to evaluate pre-storm morphology (Henderson et al. 2016). The ten original locations, plus five additional locations (Fig. 1), herein are collectively referred to as "profiles," have been resurveyed every 1 to 4 months since October 2012 (Henderson et al. 2016, 2017). Data collection at the profile locations is ongoing as of December 2017. The post-

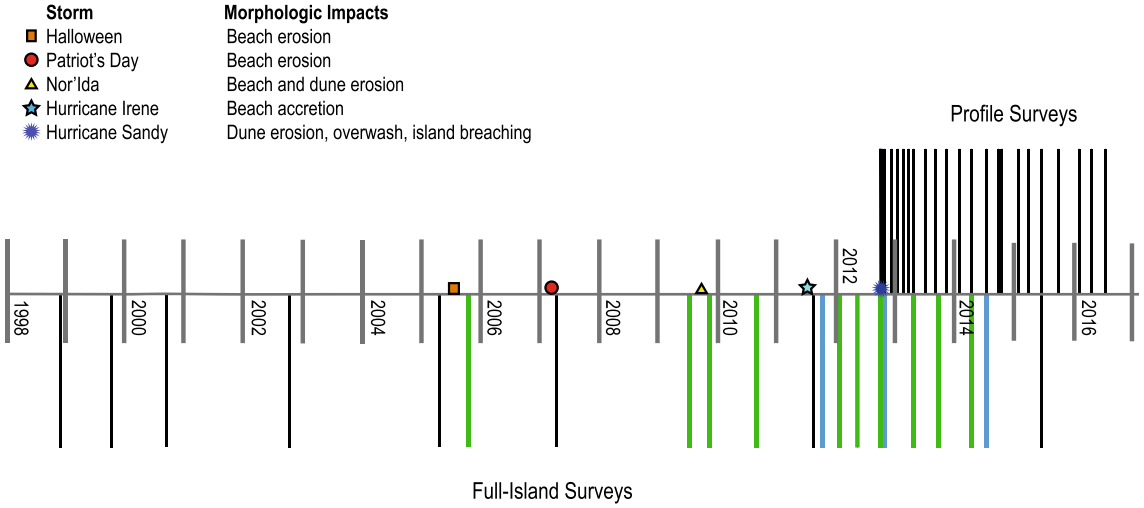

Fig. 2 Timeline of morphologic data used for Bayesian Network training and testing. Full island surveys (bottom) were intermittently collected between 1998 and 2015. Dates shown in green and blue indicate data sampled by the long-interval and short-interval datasets, respectively. Profiles were surveyed every 1 to 4 months via GPS between October 2012 and June 2016. Named storms to impact Fire Island, NY are marked on the timeline

Sandy profile dataset augments an existing historic dataset comprised of aerial photographs, an island-wide GPS survey, and 20 topographic lidar surveys collected since 1998 (see Table 1 in Supplemental Material). The historical data serve as a baseline of morphologic conditions while the profile dataset is a consistent time series designed to monitor post-Sandy recovery of the beach. Altogether, these datasets have the potential to support a robust data-based probabilistic model.

Fire Island Upper Beach Zone

We use a newly developed metric, beach change envelope (BCE), to track and predict short-term beach evolution (Hapke et al. 2015; Brenner et al. 2018). The BCE is a zone on the upper beach derived from the elevations of historic storm wave impact and bound by two location-specific elevation contours, Z_l and Z_u; for Fire Island, these elevation contours are 1.7 m (Z_l) and 2.9 m (Z_u) NAVD88 (Fig. 3). At Fire Island, the upper beach contained within the BCE is critical for island-wide accessibility via beach driving and supports endangered piping plover habitat and recreational use. Thus, predictions of sub-annual beach configuration in this zone are of value to NPS managers, community managers, and the public.

The Z_u and Z_l identified for Fire Island are above the influence of astronomical tides, making the BCE less temporally variable than the mean high water shoreline, yet also more sensitive than the more landward dunes to the seasonal changes in morphology driven by hydrodynamic conditions. In comparing the two boundaries of the BCE, Z_u is less variable than Z_l over the timescales of interest in this research. With the exception of large erosional events when Z_u position can shift landward rapidly, seaward Z_u movement is associated with longer term recovery processes spanning multiple years (Brenner et al. 2018). The position of Z_l is more dynamic and directly influenced by seasonal to annual transitions in the lower beach morphology between reflective and dissipative profiles (Short and Hesp 1982). Therefore, the seasonal fluctuations in Z_l position largely determine the BCE position (Fig. 3b) and BCE width (BCE_w). As a proxy for upper beach width, Zl is a valuable metric to rapidly quantify the short-term variations in beach morphology.

Prediction Methodology

We predict the deviation of the lower BCE contour, Z_l, from the historical average cross-shore position using a probabilistic approach (Bayesian Networks, as described in the following subsection). We subtracted each observed Z_l position within the time series from the 17-year average Z_l position (1998–2015) to calculate the Z_l deviation from average (Z_lD) using:

$$D(x,t) = \overline{Z_l}(x) - Z_l(x,t) \quad (1)$$

where x denotes the alongshore location, t denotes the survey date of observed Z_l, and $\overline{Z_l}$ is the historical average Z_l position. Using a mean-removed metric such as Z_lD provides a reference between the current beach configuration and the historical average. Positive Z_lD values reflect Z_l positions that are seaward of the mean and negative values are landward of the mean (Fig. 3b).

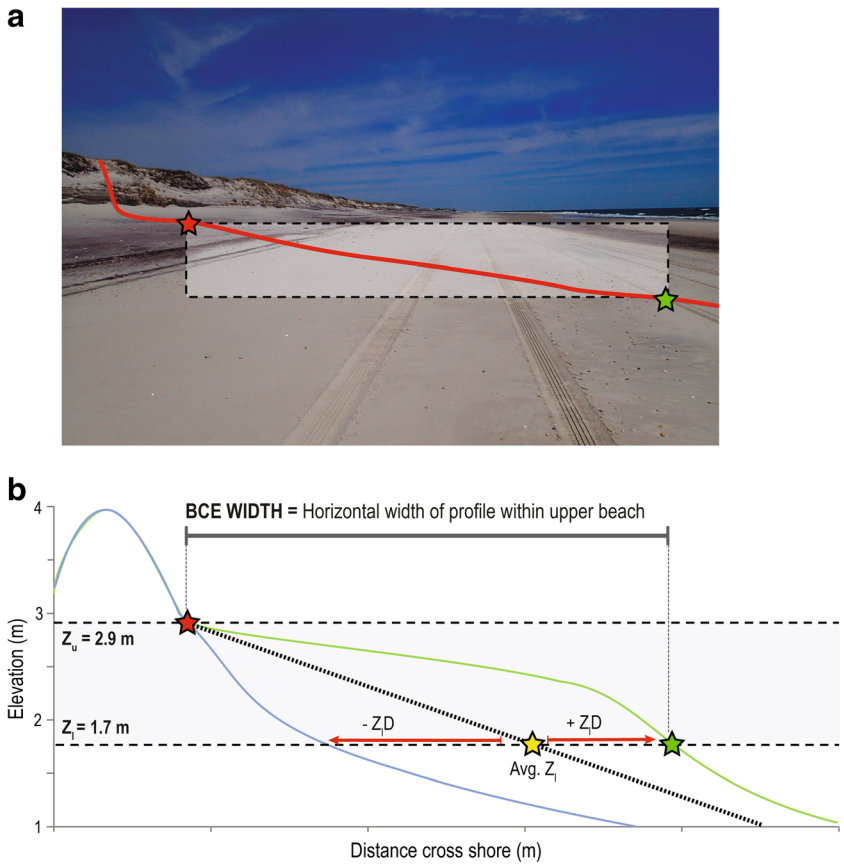

Fig. 3 **a** Photograph of the Otis Pike Fire Island High Dune Wilderness directed east. The dashed box highlights the beach change envelope (BCE). The red (Z_u) and green (Z_l) stars mark the approximate elevation boundaries of the BCE. **b** Schematic modified from Brenner et al. (2018) of an average beach profile (dashed line) and variability of beach configuration (blue and green profiles). Positive and negative Z_lD values indicate a seaward or landward deviation from average, respectively

Bayesian Networks

BNs are a form of directed acyclic graph where input variables, in the form of nodes, have causal links between variables representing the dominant processes and controls on system behavior (Jensen and Nielsen 2007); in our network, the target variable represents Z_l position. All nodes in the BN represent variables whose values are discretized to bins; when input data are continuous, bin boundaries are based on the need to balance descriptive value and predictive skill, as outlined in Plant and Holland (2011) and Fienen and Plant (2015). BNs generate predictions of a likely outcome based on knowledge, acquired through computing joint conditional probabilities of input variables using Bayes Theorem:

$$P(E_i|O_j) = \frac{[P(O_j|E_i) * P(E_i)]}{P(O_j)} \quad (2)$$

The left side of the equation is the updated, or posterior, probability of an event, given all observations($E_i|\, O_j$). The right side of the equation expresses the probability of the observations given the likelihood of the event ($O_j|\, E_i$) multiplied by the prior expectation of the event (E_i) and normalized by the prior probability of the observations (O_j). The process of learning conditional probabilities and storing those values in conditional probability tables is termed training; the marginalized conditional probabilities without constraints return the prior probabilities for each variable. The process of calculating a posterior probability of the target variable, in the form of a hindcast or forecast, is a prediction.

We present a morphologic BN (Fig. 4) to predict Z_lD, our representation of the morphologic evolution of upper beach, and a hydrodynamic BN (Fig. 5) which assimilates 18 years of deterministic model output, to produce detailed hindcasts of water levels that correspond with the survey dates of morphologic observations. Both nets are constructed using Netica software and trained with the expectation-maximization (EM) or count learning algorithms (Norsys 2010). The morphologic BN was trained with the EM method based on the robustness of the algorithm to manage cases where inputs are missing from the training data (Do and Batzoglou 2008; Norsys 2010). We chose the less computationally expensive count learning method to train the hydrodynamic BN because there were many more input datasets available for training.

We selected parameters and structure for the morphologic BN (Fig. 4) based on existing knowledge of controls on beach change, systematically testing and tailoring these components to best represent physical drivers of beach evolution at Fire Island. Building upon the conclusions and previously published sensitivity analyses of

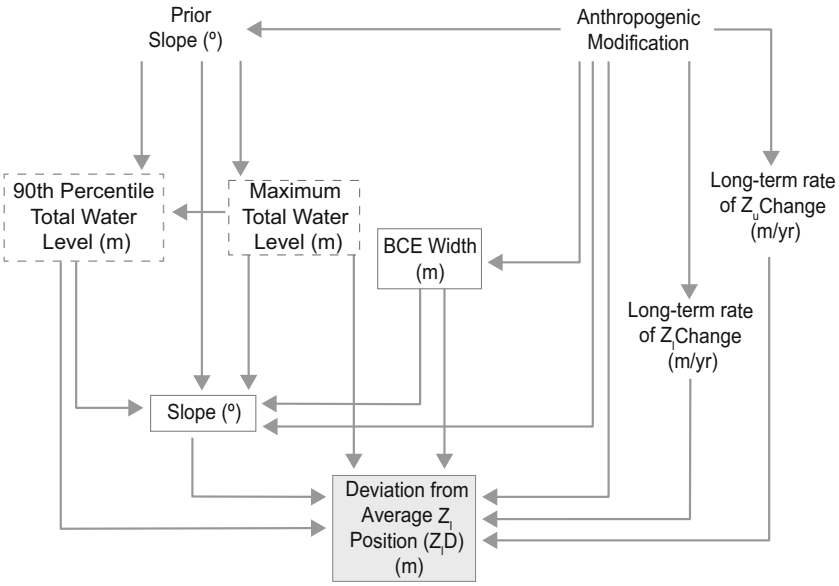

Fig. 4 Schematic of morphologic BN, displaying names and relationships between model parameters. The shaded box highlights the predicted variable, Z_lD. The solid gray boxes identify variables extracted from the end date of each survey interval. Dashed boxes designate variables that are outputs from the hydrodynamic BN

Hapke and Plant (2010), Plant and Stockdon (2012), Gutierrez et al. (2015), and Wilson et al. (2015), we included parameters to reflect oceanographic conditions such as total water level (η^{98}), historical behavior of the beach (long-term change rates of Z_u and Z_l), beach morphology (slope and BCE_w), and alongshore variability in anthropogenic modification (AM) of beach morphology. The morphologic data and the oceanographic conditions were compiled into casefiles for the BN by paired survey dates that define a survey interval. From these pairs, morphologic data (BCE_w, slope, Z_lD) were extracted from the start or end of a survey interval and the oceanographic conditions were parameterized from a time series spanning the survey interval.

Anthropogenic modification class (AM) and long-term change rates of Z_u and Z_l (Z_uC and Z_lC) are indicative of large-scale processes relating to sediment dynamics over years to decades. Collectively, Z_u and Z_l linear regression rates (Z_uC and Z_lC) and AM highlight alongshore differences in natural sediment availability and beach management practices, which can have a direct impact on upper beach width (BCE_w) and Z_l position. The hydrodynamic drivers, maximum total water level (η^{98}_{max}) and the elevation of the 90th percentile of total water level (TWL^{90}), represent seasonal and storm-event oceanographic conditions which control beach evolution over days to months. Beach conditions at the beginning of each survey interval are represented by prior slope. BCE_w, slope, and Z_lD are extracted from the survey interval end date (Fig. 4).

The available data that inform the morphologic BN span a range of density in time and space. Full island topographic data provided spatially dense but temporally limited

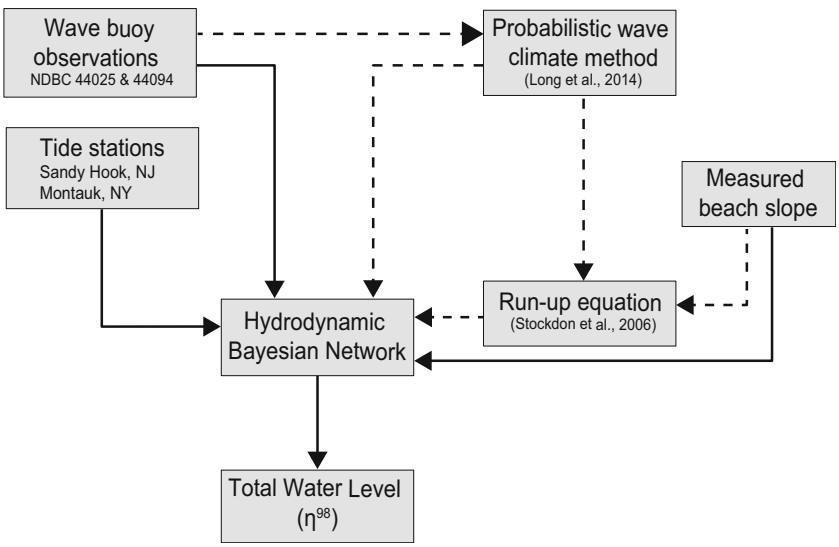

Fig. 5 Flow chart of steps to integrate hydrodynamic and morphologic data into a BN to predict total water level. Dashed line connections indicate steps to train the hydrodynamic BN and solid lines indicate steps used both in training and hindcasts of total water level. See Supplemental Material for hydrodynamic BN structure

observations while profiles collected between October 2012 through June 2016 (Fig. 2) are spatially limited, but temporally dense (Hapke et al. 2013; Henderson et al. 2016, 2017). Topographic data derived from lidar (aerial and terrestrial), photogrammetrically processed historical aerial photos, or GPS converted to a digital elevation model were extracted at cross-shore locations spaced 50 m alongshore, herein referred to as "transects." The transect data capture a range of morphologic conditions: five datasets were collected in response to a named storm (Fig. 2), three datasets collected after Hurricane Sandy and the winter of 2013 capture multi-year recovery, and the remaining datasets are classified as intermediate. The survey intervals for available transect data span up to 26 months; however, we limited model training and testing to case files with survey intervals with a maximum of 1 year. This was done to minimize uncertainty of measured prior beach slope, which was used to calculate η^{98} and assumed to remain constant through the time series of each η^{98} hindcast. The transect survey intervals were classified as either long-interval (between 6 and 12 months) or short-interval (less than 3 months: August—October 2011; October—November 2012; April—June 2014) and these classifications will be used to refer to these time intervals throughout the paper (Fig. 2). Methods to extract parameters from source datasets are explained in the Supplemental Material. Table 1 displays the nine variables used within our morphologic BN, bin discretization, and input uncertainty.

We used a separate BN to hindcast time series of total water level (η^{98}) (Fig. 5) in order to generate maximum total water level (η^{98}_{max}) and 90th percentile total water level (TWL^{90}) as inputs to the morphologic BN. The hydrodynamic BN assimilates offshore wave observations, tidal and beach slope data, and results of hydrodynamic and spectral wave modeling. The hydrodynamic and spectral wave modeling data begins with the US East Coast (5 km grid cells), scales down to resolve the Fire Island nearshore (5–40 m grid cells) (Warner et al. 2017; Safak et al. 2017), and covers 18 years between 1994 and 2012. A parametrization of measured tides, wave set-up, and swash (η^{98}; Stockdon et al. 2006) is often used to predict storm-scale impacts to the beach and dunes (Stockdon et al. 2007). During fair-weather conditions, η^{98} elevation can be used to approximate dry beach width (i.e., distance between the water line and dune toe) which is known to influence beach and dune recovery processes through cross-shore eolian fetch distance (Davidson-Arnott and Law 1996; Delgado-Fernandez 2011). Therefore, we expect η^{98} to be an informative parameter to relate to the beach morphology during both calm and energetic wave conditions.

We used the hydrodynamic BN as a means to evaluate a wide-range of storm and fair-weather wave conditions, which in turn allowed us to represent uncertainty in observations, model output, and the run-up parameterization (Stockdon et al. 2006), herein referred to as S2006. The nodes in the hydrodynamic BN were selected to reproduce S2006 and η^{98} calculation. Figure 5 illustrates the principle steps of integrating wave, tidal and morphologic data for training and hindcasting with the hydrodynamic BN (Plant et al. 2014). To train the BN, observations from the offshore buoy and deterministic model output were condensed into a database (Long et al. 2014) which describe the most likely offshore and nearshore wave conditions. The nearshore wave height and period from the database were combined with measured beach slope within S2006 and measured tide was added from the nearest tidal stations (Montauk, NY and Sandy Hook, NJ) to calculate η^{98}. This process was repeated for approximately 8.5 million joint combinations of wave, slope, and tidal observations to train the BN for numerous hydrodynamic scenarios. Additional details regarding the model parameters and BN training are outlined in the Supplemental Material.

The hydrodynamic BN produces time series hindcasts of η^{98} at less than 100-m alongshore spacing at hourly intervals for a pair of dates corresponding to the morphologic survey intervals. To generate hindcasts of η^{98}, a time series of offshore waves, tide observations, and a measured beach slope are supplied to the hydrodynamic BN. The peak elevation of the predicted η^{98} time series (η^{98}_{max}) and the 90th percentile η^{98} (TWL^{90}) are used as inputs to the morphologic model that predicts Z_lD. An advantage of TWL^{90} is that the values summarize the majority of wave conditions during a survey interval, whereas η^{98}_{max} represents the peak condition. Thus TWL^{90} represents fair-weather and beach-building conditions included in the morphologic BN, while η^{98}_{max} represents the most energetic wave conditions observed during a given survey interval.

Experiment Design

BN training is the estimation of conditional probabilities of input data, whereas the prediction generates the posterior probability of an event, given a combination of input observations. In making a prediction, the observations of the predicted variable (Z_lD) are withheld from the model at the time of prediction, while the other predictor variables are supplied to the trained model to produce an expected likelihood of an outcome. There are six binned Z_lD outcomes in the morphologic BN that range from much more seaward than average (40.0–75.0 m) to much more landward than average (− 200 to − 30 m) Z_l position (Table 1). The number and spacing of Z_lD bins were selected to disperse observations among bins, ensuring the variety of scenarios captured by the data were represented within the BN training. For model calibration, the testing data comprises a portion or all of the training data, whereas for validation, the testing data are not contained within the training data. In both calibration and validation, the testing data are compared to the prediction to assess predictive

Table 1 Variables in the morphologic Bayesian network, input error term, and discretization of bins

Variable	Error	Bin ID					
		1	2	3	4	5	6
Prior slope (°)	0.045	0.0–0.05	0.05–0.1	0.1–0.31	–	–	–
Slope (°)	0.045	0.0–0.05	0.05–0.1	0.1–0.31	–	–	–
Maximum total water level (m)	0.2	1.0–1.7	1.7–2.9	2.9–4.0	4.0–6.0	–	–
90th Percentile TWL (m)	0.2	0.0–1.25	1.25–3.0	3.0–6.0	–	–	–
BCE width (m)	2.5	0.0–30.0	30.0–60.0	60.0–50.0	–	–	–
Anthropogenic modification	0	Minimal	Indirect	Direct	–	–	–
Z_u change (m/year)	0.4	− 4.0–− 1.0	− 1.0–0.0	0.0–1.0	1.0–5.0	–	–
Z_l Change (m/year)	0.7	− 4.0–− 1.0	− 1.0–0.0	0.0–1.0	1.0–5.0	–	–
Z_lD (m)	2.5	Much more landward − 200.0–− 30.0	More landward − 30.0–− 8.0	Average − 8.0–8.0	More seaward 8.0–25.0	Moderately more seaward 25.0–40.0	Much more seaward 40.0–75.0

skill. We designed three validation experiments to (1) predict Z_lD at the transects, spaced at 50 m, spanning a range of land-use and observed coastal changes; (2) forecast post-Sandy beach recovery at three available dates (October 2013, April, and June 2014); and (3) identify data requirements for BN training to produce confident and accurate predictions between datasets comprised of a range of spatial and temporal resolutions.

For the first experiment, the alongshore predictions, we trained the BN with observations located at the spatially dense transects (Fig. 1) while the observations from one transect were withheld from training as testing data. This training and testing sequence was repeated for 850 transect-specific iterations. The topographic data used in this experiment comprised storm and beach building intervals (Fig. 5); therefore, we could evaluate the BN predictions across a range of morphologic change scenarios. It is important to note that because observations were withheld based on location, as opposed to date, training data and testing data were derived from coincident survey intervals. The implications of this are considered in the "Discussion" section. In the second prediction test of post-Sandy beach change, the BN was trained with transect data from 2005 through April 2013 and generated predictions for three datasets (October 2013, April, and June 2014) that recorded beach recovery at 6, 12, and 14 months following Hurricane Sandy and the winter storms of 2013. In the third set of predictions, we tested if data collected at different locations and over intervals of 1–12 months could adequately train a BN for dissimilar datasets. We trained the BN with long-interval transect data, short-interval transect data, or GPS profiles and cross-predicted between the three data subsets. The short-interval (1–4 months) transect data is a subset of the spatially dense transect data and was designed to be a bridge between the temporal scales of the long-interval transect (6–12 months) and short-interval (< 4 months) profile datasets.

Prediction Evaluation

We used several common statistical metrics including weighted skill, accuracy, and log likelihood ratio (Plant and Stockdon 2012; Fienen and Plant 2015; Gutierrez et al. 2015; Wilson et al. 2015) to evaluate the ability of the model to generate accurate predictions of morphologic condition and to balance uncertainty with prediction resolution (Table 2). Weighted skill uses the amount of variance within the Bayesian prediction (i.e., how broad the probability distribution is) (Plant et al. 2016), and gives more confident predictions greater weight in the summation (Table 2). For our model, we consider a high skill value as 0.50 or above which indicates the prediction explains at least 50% of the observed variance in Z_lD (Plant and Stockdon 2012). Accuracy is a simple measure of whether the predicted most likely outcome matches the bin of observed Z_lD. Accuracy can be quantified by a binary number (0 or 1) for an individual prediction ($N = 1$) or as a percentage of correct predictions over a set ($N > 1$) (Table 2). In probabilistic predictions, it is possible that all bins are predicted to be equally likely. When this occurs, the prediction is considered accurate because the observation falls within a predicted bin, although highly uncertain because all outcomes are equally likely. Predictions made with likelihood above 0.40, a threshold that is 2.5 times greater than uniform distribution, are considered a confident prediction for our BN. Similarly, accuracy above 0.40 is considered to be a high value because the percentage of correct predictions is over 2.5 times higher than the model would achieve from "guessing." In addition to the accuracy metric described above, log likelihood ratio (LLR) quantifies the combined accuracy and uncertainty for each discrete prediction. LLR rewards the model for making an accurate prediction with higher likelihood than the prior and penalizes the model when the prediction is accurate (i.e., the observations matches the predicted bin) but is predicted with

Table 2 Prediction metrics

Metric	Equation	Variables	Interpretation
Weighted skill	$1-\frac{\sum\alpha^{-2}\ [y-\hat{y}]^2}{\sum\alpha^{-2}\ [y]^2}$	$\hat{y}$: predicted probability distribution y: the observed value	0.0 to 1.0, with 1 being highest skill High values demonstrate accurate and confident predictions
		α: uncertainty factor associated with each prediction input term The summation is over all predictions	Low values indicate high variance, and low precision; accuracy can increase when predictions have a uniform distribution
Log likelihood ratio	$\log\left[p_i(E_i\|O_j)_{E_i=E_j}\right]-\log\left[p_i(E_i)_{E_i=E_j}\right]$	$p_i(E_i\|O_j)$:probability of the forecast (E_i) given the observations (O_j)in the discrete bin of the observed data ($E_i=E_j$)	Negative value usually indicate incorrect prediction
		$p_i(E_i)_{E_i=E_j}$: the prior probability of the forecast (E_i) in the observed bin ($E_i=E_j$)	Positive value usually indicate an accurate prediction with higher confidence than the prior
Accuracy	$\left[\left(\sum_{n=1}^{N} Ei_n=Ej_n\right)*N^{-1}\right]$	N: number of predictions E_i: observed bin E_j: predicted bins	0.0 to 1.0, with 1 being most accurate

lower likelihood than the prior (i.e., hedging). The lowest values of LLR occur when the prediction is very confident with a high posterior probability and inaccurate. Each prediction within a time series or across a spatial domain produces an individual LLR result which can be summed or averaged across multiple predictions to summarize the set of predictions. We present averaged LLR metrics to simplify comparison of the metric between datasets with different numbers of observations.

Results

We tested combinations of training data and testing casefiles within our model containing variables of beach state (Z_lD, slope, BCE_w), historic behavior (Z_uC; Z_lC), oceanographic conditions (η^{98}max; TWL^{90}), and anthropogenic modification of beach morphology (AM). In this section, we present results from the three experiments designed to sample and predict the total morphologic dataset (Fig. 2) by alongshore location, by date (pre- or post-Hurricane Sandy), or temporal and spatial data density.

Alongshore Predictions

Predictions of Z_lD position were produced for time series of beach change at the 850 alongshore transects previously described. Each transect was represented by 5–12 observations for each variable in the morphologic BN. The number of observations per location varied due to differences in alongshore coverage of individual surveys and the opening of the Wilderness Breach (see Table 1 in Supplemental Material). An example of a location-specific prediction (Fig. 6) shows how Z_lD predictions were compared to the prior probability and observations for transect locations (Fig. 6: black dots) to validate each prediction and calculate metrics (skill, LLR, and accuracy). The example shown in Fig. 6 was selected based on the presence of infrastructure and is a location of interest to the NPS.

At Sailor's Haven (Fig. 6b), the model accurately predicted the observed Z_lD position for 65% of the time series. The most likely outcome for each date was predicted with a likelihood above our confidence threshold of 0.40 (see "Prediction Evaluation" section), with a few dates exceeding 0.66 likelihood. The BN correctly predicted Z_lD position for two surveys with different observed morphologic conditions—more seaward than average (August 2010) and more landward than average (November 2012)—with the highest likelihoods (> 0.66) in the time series. Four dates between October 2011 and October 2012 were incorrectly predicted. On average, accurate and confident predictions at this location produced high values for metrics including skill equal to 0.63 and average LLR of 0.13.

The time series of Z_lD predictions at all transects, including the example from Sailor's Haven, were compiled and analyzed by alongshore position, as well as temporal trends and three classifications of beach state. Figure 7 is arranged such that each column is a time series of most likely Z_lD at a transect and the rows are the compiled alongshore predictions for each survey interval end date. To simplify the presentation of six Z_lD bins and confidence levels, the predictions are displayed (Fig. 7) as a landward deviation (red) or seaward (gold) deviation or approximately average (blue) Z_lD position. The color scale indicates the confidence in the prediction (Fig. 7). The following paragraphs will present a summary of these alongshore predictions highlighting trends in predicted Z_lD position and where and when predictions were made with confidence versus high uncertainty.

Z_4D predictions at individual transects oscillated through time between landward, average, and seaward deviations. As

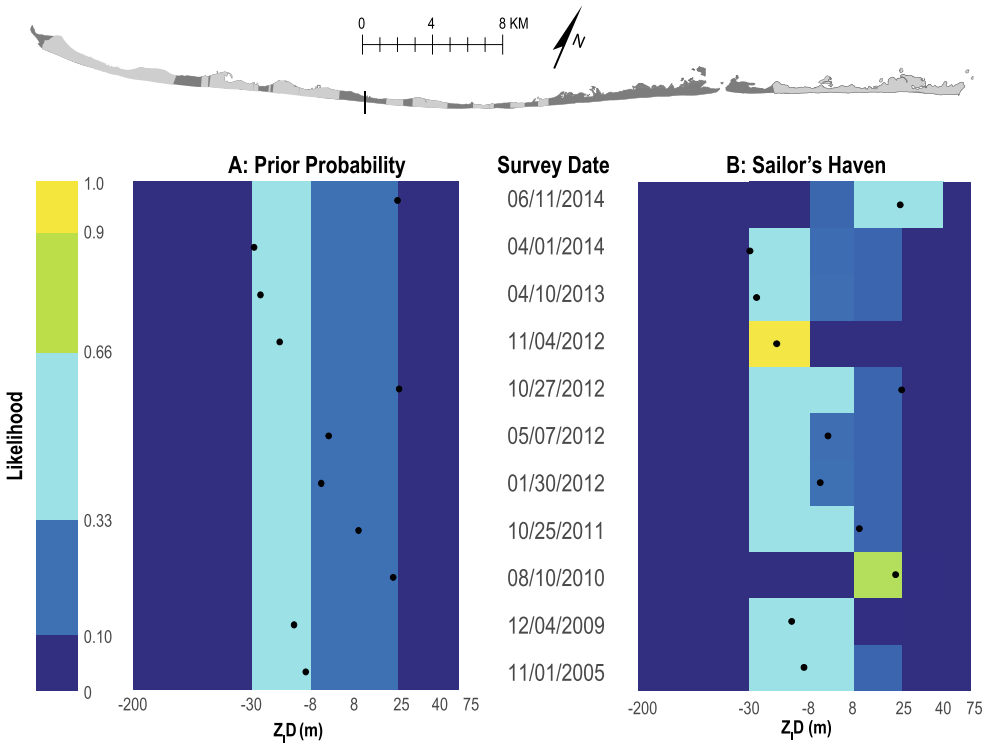

Fig. 6 Plots displaying $Z_l D$ probability for prior (**a**) and posterior probability for an example alongshore prediction at Sailor's Haven (**b**). Warm colors indicate higher predicted likelihood and cool colors indicate lower likelihood in each $Z_l D$ bin. Black dots are observed $Z_l D$ position through time. **b** Overlap of the observation and the warmest color per row in (**b**) indicates an accurate prediction. Dark gray locations on the map mark NPS tracks. Sailor's Haven is marked with the black dash

a first-order evaluation of model ability, this result demonstrates that the model is capable of predicting dynamic beach morphology beyond the prior most likely condition (e.g., Fig. 6a), which is a landward deviation from average ($Z_l D$ −30 to −8 m). Specifically, of the 9825 individual predictions, the BN predicted a landward deviation for 57%, an average configuration for 25%, and seaward deviation of $Z_l D$ for 18%. This result can be compared to the prior probabilities of 0.43 for a landward deviation, 0.31 for an average configuration, and 0.26 for a seaward deviation (Fig. 6a) to demonstrate that the prediction is not simply reproducing prior probabilities.

The alongshore predictions were also analyzed by beach state—post-storm, recovery, or intermediate. In each of the four post-storm surveys (Fig. 7), the BN predicted a landward deviation for 80–90% of transects; less than 5% of locations for each post-storm survey were predicted as a seaward deviation. Specifically, in the prediction of upper beach position following Hurricane Sandy (November 2012), Z_l was predicted to have a seaward deviation at less than 2% of transects—the lowest percentage of the post-storm predictions. In the recovery intervals, following Irene and Sandy recovery predictions differed. Predictions for the recovery intervals after Hurricane Sandy were more variable alongshore and fewer locations were predicted with confidence (> 0.40 likelihood) than post-Irene recovery in 2011. In the post-Irene recovery interval in October 2011, 78% of all transects were predicted to have an average $Z_l D$ with a notable division of predictions at 39.5 km alongshore distance (ASD), approximately the boundary of the Wilderness and Smith Point County Park. West of the boundary, 89% of the island was predicted to be in an average configuration, while 96% of transects in Smith Point County Park were predicted as a landward deviation from average. Predictions for the intermediate survey intervals ranged from prominently seaward (August 2010) to highly variable alongshore (October 2012). For August 2010, the BN confidently predicted a seaward deviation from average for 83% of transects. The three intermediate intervals in 2012 were less consistently predicted as landward, average, or seaward deviations. In particular, transects from 22 to 32 km ASD were predicted with variations between landward, average, or seaward deviations over small spatial scales.

For all alongshore predictions, 77% of predictions were made with a likelihood above 0.40, which, as stated earlier, was considered a confident prediction for our BN. Notably, every transect was predicted with a 0.40 likelihood for at least one date in the time series, meaning that not a single transect was invariably predicted with low confidence. Additionally, 15% of transects in the alongshore predictions, mostly located in the central and eastern zones of the island (12.5–27.5 and 31.5–38.5 km ASD), were predicted with confidence above 0.40 likelihood for all survey dates in the time series. The tract of NPS land between 27.5 and 31.5 km ASD, which is comprised of beaches fronting the Watch Hill ferry terminal and western portion of the Wilderness, was predicted with lower confidence than the surrounding transects. The reduced confidence of predictions in this area was apparent in the October 2013 and 2014 survey intervals and can be informative for NPS management planning. Throughout the time series,

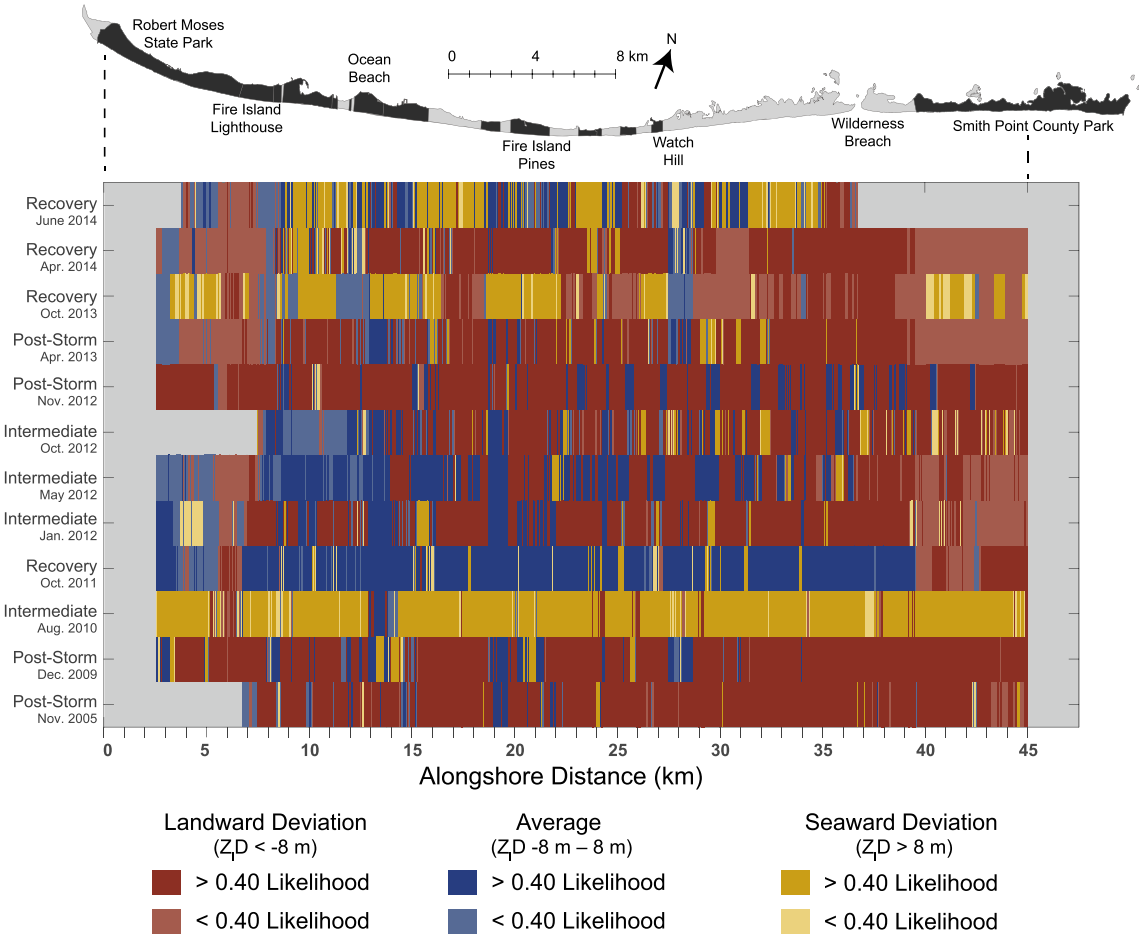

Fig. 7 Most likely Z_lD predicted at alongshore transects separated by survey date. Darker colors indicate a confident prediction above 0.40 likelihood. For simplification, landward or seaward deviation bins are displayed together. A landward deviation is comprised of two Z_lD bins, average is comprised of one bin, and seaward deviation is comprised of three bins. Gray space indicates locations lacking input observations to produce a prediction

prediction confidence tended to be lower on the eastern and western ends of the study area. For survey intervals through 2012, the predictions were confident (> 0.40 likelihood) for at least 70% of transects. Meanwhile, the predictions made for 2013–2014 had less than 70% predictions above 0.40 likelihood. We consider whether aspects of the model, data availability, or physical processes may explain the spatial and temporal variability of prediction confidence in the "Discussion" section.

The island-wide metrics (Fig. 8) summarize the predictions of Z_lD time series at 850 transects, including the example location (Fig. 6). Of the 9825 individual predictions shown in Fig. 7, 8482 were validated with available observations—56% of Z_lD positions were accurately predicted and 81% had a positive LLR results. The full island average LLR and standard deviation averaged over all predictions was 0.14 ± 0.06, indicating that the island-wide results were an improvement over the prediction capability using only the prior information. Skill averaged across all transects was 0.52. Full island prediction metrics summarized in Fig. 8 demonstrate that there was substantial alongshore variability in LLR, skill, and accuracy values. The range of LLR at any transect are visualized by the length of vertical gray bars in Fig. 8a, wherein at individual locations, LLR values vary through the time series of observed Z_lD positions. For example at Sailor's Haven (Fig. 6b), individual LLR values ranged from − 0.25, indicating a confident but incorrect prediction for October 2011, to 0.57, indicating a confident and correct prediction for August 2010. Across the island, the minimum accuracy value was 0.1 and minimum skill was near 0.0 while the maximum for both metrics approached 1.0. Within the alongshore skill results (Fig. 8b), some spatial patterns are apparent. In the area of a historic inlet and the present location of the Wilderness Breach (35–40 km ASD), individual LLR values at two transects were less than − 1.0, and individual and spatially averaged skill were below 0.2, which are among the lowest metrics along the island. Transects in the western part of the island (0–5 km ASD) produced the highest skill values and consistently positive LLR values, exceeding 1.0 at many transects, which is above the island average.

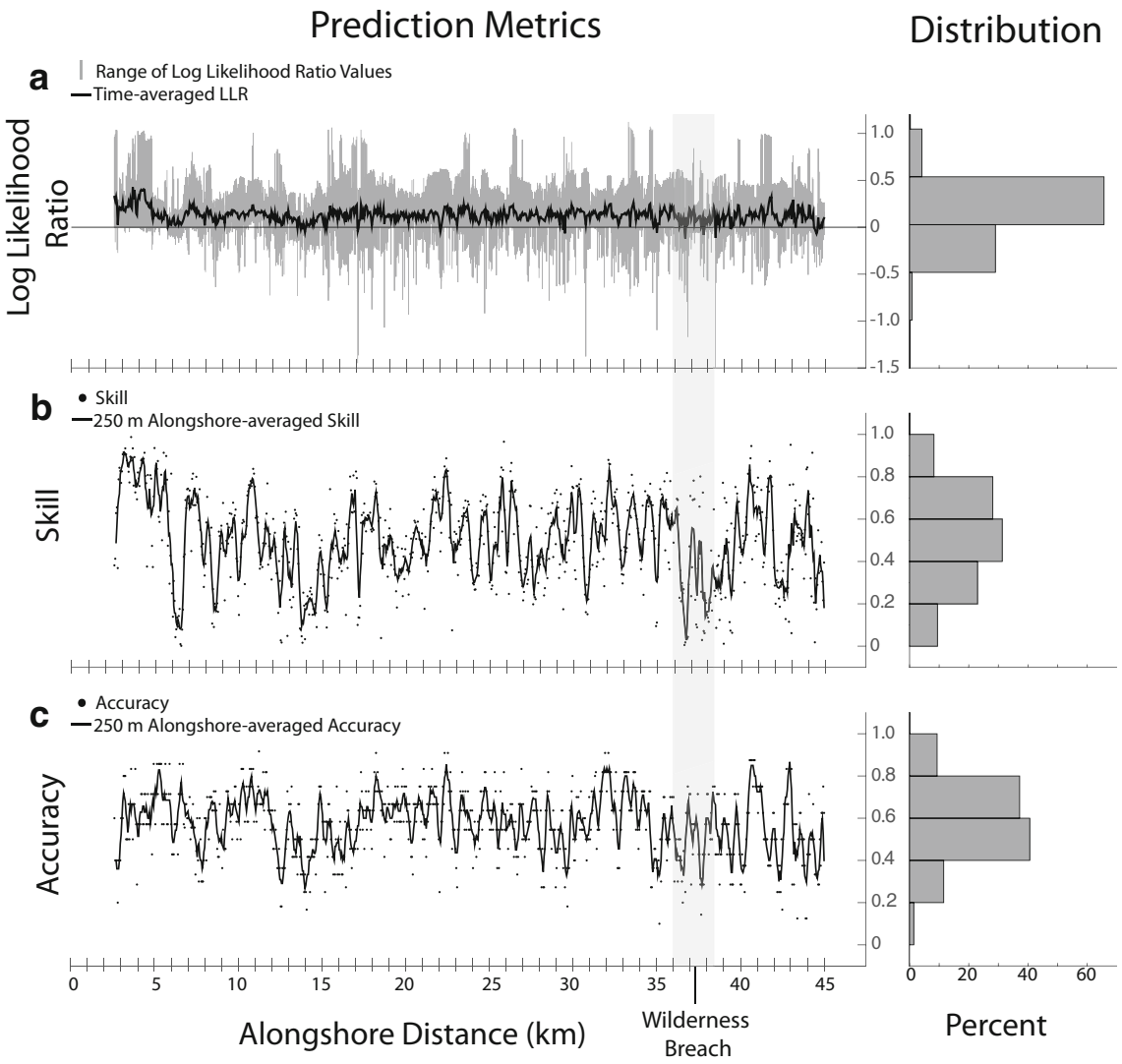

Fig. 8 Alongshore prediction metrics at transects, spaced 50-m along Fire Island. **a** Vertical lines demonstrate the range of values of log likelihood ratios for predictions at transect locations; the time-averaged LLR per transect (black line) is positive at all but 30 locations. **b** Weighted skill (dots). The black line is a moving average of 250-m (5 transects) alongshore. **c** Accuracy (dots). The black line is a moving average of 250-m (5 transects) alongshore

Predicting Post-Sandy Recovery

In the second experiment, we used the morphologic BN to predict the position of Z_lD at transect locations for three dates, all after Hurricane Sandy: October 2013, April 2014, and June 2014. For the survey interval ending in October 2013, approximately 1 year after Hurricane Sandy, the model predicted Z_lD position to be average or more seaward than average position at 77% of transects (Fig. 9b). Island-wide, the prediction for October 2013 has the best overall metrics as compared to the April and June 2014 including accurate predictions at 51% of transects, weighted skill of 0.17, and average LLR of 0.19. There are several notable zones of confident and less confident predictions. The first zone, between 18.5 and 22 km ASD, Z_lD was predicted with likelihood above 0.40, and select locations exceeding 0.66, to be more seaward than average and observations (Fig. 9: black dots) show them to be accurate. The second zone, 9.5–11.4 km ASD, showed 78% of transects predicted to be more seaward than average, with likelihood greater than 0.40, for Z_lD, validated with observations. In a western zone (6–7.5 km ASD), the model was less confident and less accurate; there was between 0.30 and 0.40 likelihood that the Z_lD would be average or more landward than average for each transect, and the observations show that the Z_l positions were actually more seaward or moderately more seaward.

In April 2014, the model predicted that Z_lD at 40% of locations would be average, 52% of transects would be more landward than the average, and the remaining locations (8%) were predicted to be more seaward than average (Z_lD 8–25 m). Two sections of beach (12.5–15.5 km ASD and 16–19.5 km ASD) showed predictions were confident and

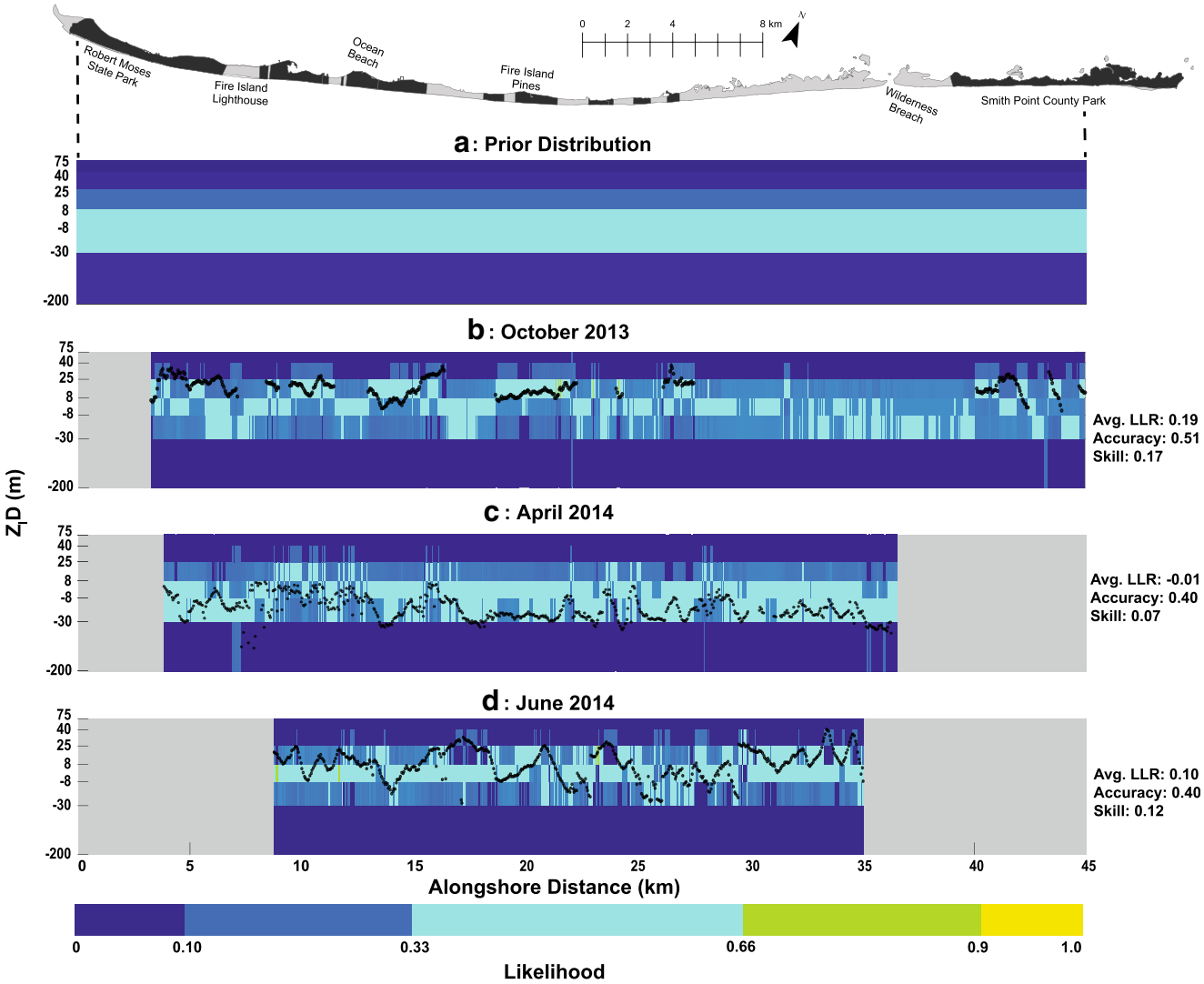

Fig. 9 Prior probability distribution (**a**) and predicted Z_lD probability for October 2013 (**b**), April 2014 (**c**), and June 2014 (**d**). Black dots display observed Z_lD for each survey date. Summary metrics for the three predicted dates are listed at the right. Locations lacking data (black dots) to validate a prediction are not included in the calculation of evaluation metrics. Areas classified as direct modification, based on nourishment frequency and infrastructure, are shown in black in the inset map

inaccurate; results showed greater than 40% likelihood that Z_lD would be an average configuration; however, Z_lD observations showed that the upper beach position was more landward than average. By contrast, in the Wilderness (31–35 km ASD), predictions were both accurate and confident; Z_lD was predicted to be more landward than average with likelihoods nearing 0.50, and validated by observations. Z_lD position closer to the Wilderness Breach (35–36 km ASD) was predicted to be more landward than average but Z_l in this area was actually much more landward than average.

For June 2014, within the western to central part of the island, 8.5–20 km ASD, the BN consistently predicted average position for Z_lD with likelihoods from 0.33 to 0.85. However, the observations varied from more landward than average to moderately more seaward than average and the model was incorrect at 65% of transects between 8.5 and 20 km ASD (Fig. 9D). In the eastern portion of the island (30–35 km ASD), observations showed that the Z_lD was accurately predicted as average or as more seaward than average at 55% of locations. The overall accuracy for June 2014 was 0.40, but correct predictions were concentrated in the east and many locations in the west were incorrectly predicted. A skill value of 0.12 and the positive LLR values indicate an overall improvement of the prediction over the prior (Fig. 9d).

Evaluation of Training Data Requirements

In the third set of predictions, we used combinations of data subsets to explore the value of temporal or spatial density within morphologic data to inform a BN. This experiment aims to provide insight to data acquisition and necessary

resolution to predict short-term upper beach change. Spatially dense transect data were subdivided by the length of survey interval into short-intervals (1–4 months) and long-intervals (6–12 months), and combined with temporally dense but spatially limited profile dataset. Therefore, the profile data and short-interval transects had similar temporal resolution and the short-interval transects and long-interval transects had similar spatial resolution.

Training the BN with profile data (Table 3; column 1) produced mixed results in predicting short- and long-interval transect data. Short-interval transect data had a skill of 0.09 and a negative average LLR value, both of which indicate a poor prediction, whereas the long-interval transects resulted in the highest accuracy (0.48) and the highest average LLR (0.05) values of the cross-validation tests. Training the BN with the short-interval transect data (Table 3; column 2) produced results with the same accuracy value (0.40) with variable skill (0.25 for profile vs. 0.03 for the long-interval). Negative values of average LLR for both predictions made with the short-interval training indicated the predictions of profiles and long-interval transects were more often incorrect or uncertain over the whole dataset.

When trained with the long-interval transect data (Table 3; column 3), predictions resulted in the best overall metrics for this experiment: prediction of the profile dataset had the highest skill (0.40), and was accurate for nearly half of the observations. Prediction of short-interval transects resulted in the second highest skill of these cross-validation tests and over one-third of observations were correctly predicted. Comparing the three metrics, the BN trained with long-interval transects predicted the observed Z_lD position at the profiles than Z_lD at the short-interval transects. We expected that evaluation metrics across the six calibration-validation tests (Table 3) would exhibit trends that mirror the similarity of spatial or temporal density of the datasets. However, cross-predictions between the profiles and long-interval transects produced the highest values of evaluation metrics and the short-interval transects reported lower combined metrics.

Discussion

The development of a probabilistic modeling approach that can incorporate observational data across multiple beach states and skillfully predict beach changes over sub-annual to annual time scales is a relevant advancement to coastal research. The morphologic BN presented here complements storm-induced morphologic change models (Plant and Stockdon 2012; Wilson et al. 2015) by advancing our ability to predict both storm impact and recovery components of beach change using a single morphologic framework. Our BN can efficiently produce probabilistic predictions of upper beach configuration, as represented by Z_lD, for storms, short-term beach building intervals, and multi-year beach recovery at spatial scales (50 m) and timescales (1–12 months) relevant to landscape and habitat management.

Alongshore Predictions: Assessment of Overall Model Function and Outcomes

Of the three experiments, alongshore predictions generated by our BN were most successful, making accurate, confident, and skilled predictions of temporal changes in the beach state when compared with observations. Generally, the BN predicted post-storm impacts as landward shifts of Z_lD, particularly after nor'easters in 2005 and 2009, and the stormy winter season of 2013. In the survey interval containing Hurricane Sandy (November 2012), predictions of Z_lD position show alongshore variability consistent with observed overwash (Hapke et al. 2013) and storm impacts. For example, predicted landward movement of Z_lD on the western portion of the island (Fig. 7: Nov. 2012; 3–8 km ASD) corresponds to observed sheet-like overwash of dunes. Irregular patterns of overwash were observed in the eastern beaches, corresponding to landward and average alongshore fluctuations in predicted Z_lD position. By contrast, for non-storm intervals, average or more seaward shifts were predicted. This result follows expected behavior for beach recovery when beach building material moves onshore in the days and weeks following a storm. Intermediate periods generally showed greater alongshore variability than either recovery or storm periods, likely reflecting the influence of seasonality and human modifications on beach behavior. As noted in the results, the combined metrics for the alongshore predictions are considered high, reporting positive values for alongshore average LLR along with skill and accuracy above 0.5, with a few alongshore exceptions that will be explored later in this section.

The overall success in generating accurate alongshore predictions is somewhat expected given the model design and training. To make predictions, a specific survey interval at one transect location was withheld, meaning that data at all other transects from the same survey interval were available for training and to inform the model. This meant that each alongshore prediction had a larger training dataset than any other experiment, comprised of approximately 10,000 observations. Extensive training datasets such as this provide the best opportunity for the model to maximize the number of unique conditional probabilities learned by the BN (Palmsten et al. 2014). Due to transect density, however, this approach incorporates inherent spatial correlation often found in predictions of coastal morphologic behavior (Hapke et al. 2010). In their assessment of morphologic change over time scales of greater than a decade, for example, Lentz et al. (2013) found that spatial correlation of morphologic features occurs over approximately 250 m alongshore lengths at Fire Island. Therefore, it is likely that some of the

Table 3 Prediction results for transect and profile cross-validation

Testing data	Training data								
	Spatially limited profiles (1–4 months; $N = 320$)			Short-interval transects (1–4 months; $N = 2358$)			Long-interval transects (4–12 months; $N = 7467$)		
	Avg. LLR	Skill	Accuracy	Avg. LLR	Skill	Accuracy	Avg. LLR	Skill	Accuracy
Profiles	x	x	x	-0.01 ± 0.37	0.25	0.40	0.04 ± 0.24	0.40	0.47
Short-interval transects	-0.01 ± 0.27	0.09	0.42	x	x	x	0.04 ± 0.24	0.27	0.37
Long-interval transects	0.05 ± 0.2	0.08	0.48	-0.03 ± 0.30	0.03	0.40	x	x	x

success in the alongshore predictions is attributable to spatial dependence between predicted and training transects that is unaccounted for in our methodology, and is a component to test in future work.

Specific parameters in the modeling framework serve to further improve alongshore predictions by capturing distinctions in behavior at different locations and for different oceanographic forcings. Gutierrez et al. (2015) and Wilson et al. (2015) demonstrated that AM is a valuable BN parameter for predicting alongshore variability in the morphologic beach state on populated barrier islands that is not well represented by other parameters. In agreement with prior results (Gutierrez et al. 2015; Wilson et al. 2015), our model predictions demonstrate the influence of AM reflected in predictions and skill, wherein wider beaches fronting communities and Robert Moses State Park were accurately predicted post-replenishment (Fig. 7 wider beaches at ASD13; ASD 19, and 27) with high skill values (Fig. 8). In addition, the parameters of beach slope and width improve the confidence and skill of the model in predicting Z_lD across a range of disparate recovery paths, such as in the cases of Hurricane Irene and Hurricane Sandy. Unlike Hurricane Sandy, Irene resulted in widespread upper beach accretion (Brenner et al. 2018). Because the prior beach slope, which is calculated at the start of the survey interval immediately following Irene, informs the prediction of beach configuration, our 2-month recovery predictions after Irene show wider beaches with steeper slopes than other post-storm recovery predictions, such as Hurricane Sandy. Furthermore, by accounting for high wave energy through $\eta^{98}{}_{max}$ and TWL^{90}, the model is able to differentiate between storm intensity and thus expected morphologic change; Hurricane Sandy was correctly predicted to be the most erosional (via landward shift of Z_lD) of any of the five storms in the dataset.

The long-term change parameters included in the model reflect geospatial trends due to geological controls on the system that are likely to help refine predictions of beach behavior (Gutierrez et al. 2011). A body of literature has documented shoreline stability in central Fire Island attributable to erosion of a lobe of Pleistocene outwash sediment during the Holocene marine transgression (Schwab et al. 2013). The west features erosional hotspots within a long-term elongating spit due to a combination of sediment availability and shelf morphologic variability, while the east is characterized by measureable transgression via overwash and inlet creation due to a sediment-starved shoreface (Leatherman 1985; Schwab et al. 2000; Schwab et al. 2013; Lentz et al. 2013). Dune and beach behavior that is in part connected with these geologic framework regions has been documented in interannual, decadal, and centurial studies at Fire Island (Hapke et al. 2010; Lentz and Hapke 2011; Lentz et al. 2013; Schwab et al. 2013; Hapke et al. 2016). Regional patterns of centennial-scale coastal change are similarly evident in alongshore predictions and confidence of Z_lD (Fig. 7), for example, by predicting a more stable central reach with high confidence, as compared to wider trending beaches to the west, and intermittently eroding and accreting beaches further east.

We find a more complicated interpretation of predicted Z_lD in the area surrounding the Wilderness Breach. Following Hurricane Sandy, predictions on the eastern side of the Wilderness Breach (36.5 ASD) show a largely consistent landward deviation in the eastern portion of the island from October 2013 to June 2014 in agreement with the transgressive behavior historically observed. The prediction of landward deviations can also be explained in part by limited input data to the model; except for partial spatial coverage in October 2013, morphologic observations were not collected east of the breach during the post-Sandy period. Consequently, many transects in the eastern reach of Fire Island lacked several inputs (e.g., BCE_w, slope, wave parameters) in the test case. In cases with reduced-input data, the BN is less confident than when the test case has all inputs, and relies more heavily on long-term rates of change (Z_uC and Z_lC) which capture the eroding trends in the eastern reach of Fire Island. As a result, the Z_lD posterior probability closely resembles the prior most likely condition, a landward deviation from average. By contrast, the location of the Wilderness Breach had ample input data and persistently poor skill, suggesting the existing model parameters do not provide sufficient information to accurately predict behavior at this location. Although the BN predicted likelihoods above 0.40 at the location of the breach, both skill and accuracy are among the

lowest along the island (Fig. 8). This implies that the processes which contributed to the creation of the breach are inadequately represented by the BN.

In summary, an assessment of our alongshore predictions show that we are generally able to accurately and confidently predict beach behavior in response to storms and during recovery periods in a barrier island setting. In addition to detailed observations, our results agree with prior studies (Plant and Stockdon 2012; Gutierrez et al. 2015; Wilson et al. 2015) that show BN parameters that capture longer term trends related to the geology, as well as human modifications to the system, inform alongshore differences in behavior. However, the detailed assessment of variability in alongshore metrics provided here also helps to identify along-coast deviations in processes or behavior from those represented by our model, wherein finer-scale, more detailed modeling approaches may be best applied to generate more accurate and precise predictions. The results presented here suggest Bayesian Networks can be employed as a computationally inexpensive tool to address a variety concerns related to monitoring and management of coastal barrier and mainland beach settings, helping also to identify where new or better data, or improved understanding of coastal processes may be necessary to inform both research and decision-making agendas.

Post-Sandy Assessment: Forecasting Beach Recovery

In evaluating outcomes from our second experiment, it is important to first note that due to seasonal fluctuations and human modifications, $Z_l D$ observations over the three post-Sandy survey intervals did not demonstrate a monotonic seaward progradation of $Z_l D$ in the recovery progression (Brenner et al. 2018). The majority of our October 2013 observations were collected in the communities and state and county parks (51% direct modification, 7% indirect, 42% minimal modification; Wilson et al. 2017), to provide cross-shore profiles ahead of a planned large scale replenishment. Although the replenishment project was not yet underway, localized movement of sand and sand-bag placement on dunes was witnessed along the island prior to the October 2013 survey (Owen Brenner, personal communication, May 25, 2016). This modification was captured by the profile data, resulting in a larger percentage of $Z_l D$ positions being seaward of average than other recovery intervals. By contrast, April 2014 observations captured the seasonal, post-winter signal, resulting in more depleted beaches and hence, a more landward shift of $Z_l D$ (89% of observations). June 2014 observations were collected in relatively close temporal proximity to April 2014, wherein significant changes between the periods would more likely reflect seasonal change as opposed to sustained post-storm recovery. In sum, the three survey intervals captured a complex morphologic response that included post-storm recovery processes along with seasonal fluctuations and ongoing engineering projects.

Despite the response complexity, we were able to accurately predict post-Sandy recovery with likelihoods above a uniform distribution for these three periods. The BN predicted a Z_l seaward deviation ($Z_l D > 8$ m) at 86% of transects surveyed in October 2013, accurately resolving the above-mentioned anthropogenic modifications. Although April 2014 predictions had lower skill than October 2013 (Fig. 9), an average LLR value close to zero suggests that the predicted $Z_l D$ conditions were similar to pre-Sandy island-wide observations (i.e., the prior probability). June 2014, the survey farthest in time from the training datasets, was the most successful prediction after October 2013. Here, a shorter survey interval (April–June 2014) meant that our prior slope measurement was likely representative through the end of the survey interval and the hindcast of water levels had lower uncertainty, resulting in both positive prediction metrics and high confidence. Our success in generating post-Sandy predictions shows that established BNs can continue to use an existing dataset to make predictions of future short-term beach behavior.

Worth noting here is that in this paper, we provide a comparison of Z_l position to a historical average rather than Z_l position relative to a set pre-Sandy baseline. After Sandy, there is substantial evidence that the Z_u and Z_l contours at Fire Island were translated landward substantially which is incorporated into the average Z_l position by using observations through 2015. Furthermore, although predictions are possible without adding more to the training dataset, we suggest it is important to collect data periodically that can be used as the "prior condition" to ensure confidence over prediction timescales. Best practices for developing and training BNs can be used to inform data collection or guide beach monitoring programs at Fire Island or other areas more broadly that may support data-based models.

Effects of Varying Spatial and Temporal Density of Model Input Data

Contrary to our expectation, the profile and long-interval transect end-member datasets produced the best cross-validation metrics while the short-interval transect data produced the least successful predictions in this test. The composition of the short-interval transect data may have contributed to this result. Unlike profile and long-interval transect data, which had a broad spatial distribution and temporal coverage, the short-interval transect data were heavily influenced by Hurricane Sandy. For example, when trained with the short-interval transect data, we found the prior probabilities of the short-interval data were shifted toward high values of TWL^{90} (3–6 m) and low values for slope (0–0.05°), consistent with the elevated water levels and severe erosion (i.e., flattening of

the beach) resulting from large storms such as Hurricane Sandy. Although the long-interval transect data and profile datasets also included storm intervals, the post-Sandy response comprised one-third of the short-interval transect data. In fact, differences in the TWL^{90} and slope distributions of the long-interval transect or profile training datasets (Fig. 6 in Supplemental Material) implies that the short-interval transect dataset may not represent a realistic distribution of conditions at Fire Island beaches. As a result, the skewed prior distribution of short-interval transects limited the BN to accurately predict Z_lD within the other datasets.

By contrast, the successful predictions made by the BN when trained with the long-interval transect data or the profiles can likely be attributed to generalizable prior probability for Z_lD. For the long-interval transects, the spatial density of transects and the decade-long time series of post-storm and recovery intervals within this dataset made it the most generalizable of the three subsets. These characteristics of the data led to successful prediction of short-interval transects and profile data. Similarly, the profile dataset had a generalizable prior probability for Z_lD achieved through the spatial and temporal design of the monitoring program. Specifically, the profiles sampled the geomorphic variability of Fire Island beaches by being clustered throughout the western, central, and eastern regions. The three geologic regions of Fire Island have been shown to express different patterns of barrier island evolution, ranging from a transgressive system to an actively prograding spit. The profiles are also dispersed among different zones of development which reflected different scales of anthropogenic modification within the communities and county and state parks. In addition, the surveys of spatially limited profiles were timed to capture a severe storm (Hurricane Sandy), short-term recovery, and seasonal variability, therefore the observations were not dominated by a particular hydrodynamic or morphologic condition. We therefore suggest that the spatial and temporal variability of the profile dataset compensates for a lack of spatial coverage or a longer time series, a finding that is particularly useful in designing and maintaining a cost-effective monitoring program at Fire Island or elsewhere.

Overall, the results of the cross-validation tests suggest datasets capturing a variety of beach change and hydrodynamic conditions are most important for successful prediction of upper beach change within a BN than similarity in spatial or temporal resolution of the training data. BNs are susceptible to overfitting a particular set of conditions because a BN cannot predict (1) conditions outside of pre-determined variable boundaries or (2) a set of conditions that were previously not encountered in model training. Our results illustrate that transferability of a trained BN is not solely questionable between study sites (Palmsten et al. 2014), but should also be considered when predicting conditions that are not well represented in the observational data at one location.

Most importantly, the results of our third experiment show that datasets collected at dissimilar sampling frequency can be compiled and used to predict each other with accuracy and skill values comparable to other BN models for barrier islands (Gutierrez et al. 2015). When the BN was trained with the profiles as compared to the long-interval transect data, predictions sacrificed skill (80% reduction) for a 95% reduction in the number of training data, while accuracy and average LLR metrics remain high, indicating increased uncertainty (Table 3). These results demonstrate the ability to extrapolate spatially limited but temporally dense data (profiles) to spatially dense locations (transects). The ability to integrate data across a range of collection techniques is particularly informative for researchers who want to target or optimize data acquisition; infrequent and expensive continuous topographic data can be augmented or possibly even replaced with more affordable and easily repeatable profile data.

Conclusions

In this study, we present a BN to predict beach morphodynamics on intervals up to a year and investigate BN ability to predict beach change through rigorous testing across multiple spatial scales and morphologic configurations. The results indicate that a BN containing morphologic and hydrodynamic variables trained with a robust dataset is able to predict beach change with greater confidence than the prior likelihood and can predict beach evolution resulting from storm and non-storm conditions, including beach recovery. Predictions of Z_lD position at 50 m alongshore spacing resulted in significant variability in transect-specific prediction metrics. Locations with high likelihood of a desired outcome (e.g., wide upper beach) have the potential to support decision makers in habitat and landscape planning on seasonal to 1-year time scales, while poor prediction ability highlights locations where additional observations or modeling techniques would be beneficial. Prediction metrics for three post-Sandy datasets demonstrate that pre- and post-Sandy training data were adequate for predicting post-extreme event recovery. The results demonstrate that the BN presented here is a computationally inexpensive tool to predict sub-annual beach evolution after an extreme event.

We show through cross-validation tests between end-member datasets (e.g., spatially limited, temporally dense or spatially robust, temporally sparse) that data compiled from different spatial coverages and temporal frequencies (1 to 12 months) can train a BN that is capable of making predictions with nearly 50% accuracy, or more than three times than would be predicted by the untrained model. The results suggest that regular surveys at limited profile locations are able to extrapolate to predict spatially comprehensive locations and predict upper beach change accurately, although skill is

sacrificed. Additionally, spatial variability in morphologic observations and beach configuration can balance limited temporal resolution as suggested by the metrics when the model is trained with the long-interval transect data. However, to maximize BN applicability, we recommend that training data encompass a suite of post-storm and fair-weather beach conditions. Collectively, the work suggests that BNs and their data requirements can be tailored to a specific set of predictive requirements (e.g., time horizon, confidence, accuracy) making this methodology highly applicable to a range of coastal change scenarios, easily portable to other barrier islands or sandy mainland beaches, and useful in assisting landscape and habitat management on short-term planning horizons.

Acknowledgements The authors are grateful to our partners at the National Park Service: Fire Island National Seashore. We thank USGS's Joseph Long, Cheryl Hapke, and Rachel Henderson for their help through thoughtful discussions. Rachel Henderson extracted morphologic features from many of the datasets. We thank Benjamin Gutierrez, Nathaniel Plant, and two anonymous reviewers for helpful comments and critiques. This work was supported by the National Park Service National Resource Preservation Program. Any use of trade, firm, or product names is for descriptive purposes only and does not imply endorsement by the U.S. Government.

References

ASPBA National Beach Nourishment Database, 2017. https://gim2.cbi.com/ASBPANationwideRenourishment/ [13 June 2017].

Belknap, D.F., and J.C. Kraft. 1985. Influence of antecedent geology on stratigraphic preservation potential and evolution of Delaware's barrier systems. *Marine Geology* 63 (1–4): 235–263. https://doi.org/10.1016/0025-3227(85)90085-4.

Blake ES, Kimberlain TB, Berg, RJ, Cangialosi JP, Beven JL. 2013. Tropical Cyclone Report Hurricane Sandy (AL182012) 22–29 October 2012. National Hurricane Center. Miami, Florida. 12 February 2013.

Brenner, O.T., E.E. Lentz, C.J. Hapke, R.E. Henderson, K.E. Wilson, and T.R. Nelson. 2018. Characterizing storm response and recovery using the beach change envelope. *Geomorphology* 300: 189–202.

Bruun, P. 1983. Beach scraping—is it damaging to beach stability? *Coastal Engineering* 7 (2): 167–173.

Carter, R.W.G., R.W. Johnston, J. Mckenna, and J.D. Oxford. 1987. Sea-level, sediment supply, and coastal changes: examples from the coast of Ireland. *Progress in Oceanography* 18 (1–4): 79–101.

Davidson-Arnott, R., and M.N. Law. 1996. Measurement and prediction of long-term sediment supply to coastal foredunes. *Journal of Coastal Research* 12 (3): 654–663.

Delgado-Fernandez, I. 2011. Meso-scale modeling of aeolian sediment input to coastal dunes. *Geomorphology* 306 (3-4): 230–243. https://doi.org/10.1016/j.geomorph.2011.04.001.

Do, C.B., and S. Batzoglou. 2008. What is the expectation maximization algorithm? *Nature Biotechnology* 26 (8): 897–899. https://doi.org/10.1038/nbt1406.

Field Research Facility Data Portal. 2017. http://navigation.usace.army.mil/CHL_Viewer/FRF/ [1 February 2017].

Fienen, M.N., and N.G. Plant. 2015. A cross-validation package driving Netica with python. *Environmental Modelling & Software* 63: 14–23. https://doi.org/10.1016/j.envsoft.2014.09.007.

Fitzgerald, D.M., M.S. Fenster, B.A. Argow, and I.V. Buynevich. 2008. Coastal impacts to sea level rise. *Annual Review of Earth and Planetary Sciences* 36 (1): 601–647. https://doi.org/10.1146/annurev.earth.35.031306.140139.

Gieder, K.D., S.M. Karpanty, J.D. Fraser, D.H. Catlin, B.T. Gutierrez, N.G. Plant, A.M. Turecek, and E.R. Thieler. 2014. A Bayesian network approach to predicting nest presence of the federally-threatened piping plover (Charadrius melodus) using barrier island features. *Ecological Modelling* 276: 38–50. https://doi.org/10.1016/j.ecolmodel.2014.01.005.

Gutierrez, B.T., N.G. Plant, and E.R. Thieler. 2011. A Bayesian network to predict coastal vulnerability to sea level rise. *Journal of Geophysical Research* 116 (2). https://doi.org/10.1029/2010JF001891.

Gutierrez, B.T., N.G. Plant, E.R. Thieler, and A. Turecek. 2015. Using a Bayesian network to predict barrier island geomorphologic characteristics. *Journal of Geophysical Research: Earth Surface* 120 (12): 2452–2475. https://doi.org/10.1002/2015JF003671.

Hapke, C.J., and N.G. Plant. 2010. Predicting coastal cliff erosion using a Bayesian probabilistic model. *Marine Geology* 278 (1–4): 140–149. https://doi.org/10.1016/j.margeo.2010.10.001.

Hapke, C.J., E.E. Lentz, P.T. Gayes, C.A. McCoy, R.E. Hehre, W.C. Schwab, and S.J. Williams. 2010. A review of sediment budget imbalances along Fire Island, New York: can nearshore geologic framework and patterns of shoreline change explain the deficit? *Journal of Coastal Research* 263: 510–522. https://doi.org/10.2112/08-1140.1.

Hapke CJ, Brenner OT, Henderson RE, Reynolds BJ. 2013. Coastal change from Hurricane Sandy and the 2012–13 winter storm season—Fire Island, New York, U.S. Geological Survey Open-File Report 2013–1231, U.S. Geological Survey: Reston, VA. http://pubs.usgs.gov/of/2013/1231/.

Hapke CJ, Brenner OT, Henderson RE. 2015. Quantifying the geomorphic resiliency of barrier island beaches. *Proceedings of the Coastal Sediments 2015*, San Diego, CA, 11–15 May. https://doi.org/10.1142/9789814689977_0249.

Hapke, C.J., N.G. Plant, R.E. Henderson, W.C. Schwab, and T.R. Nelson. 2016. Decoupling processes and scales of shoreline morphodynamics. *Marine Geology* 381: 42–53. https://doi.org/10.1016/j.margeo.2016.08.008.

Henderson, R.H., C.J. Hapke, O.T. Brenner, and B.J. Reynolds. 2016. *Hurricane Sandy beach response and recovery at Fire Island, New York: shoreline and beach profile data, October 2012 to October 2014: U.S. Geological Survey data series 931*. Reston VA: US Geological Survey. https://doi.org/10.3133/ds931.

Henderson, R.H., C.J. Hapke, O.T. Brenner, and B.J. Reynolds. 2017. *Hurricane Sandy Beach response and recovery at Fire Island, New York: shoreline, beach profile data, and breach shoreline data: October 2012 to September 2016*. Reston, VA: U.S. Geological Survey Data Release. U.S. Geological Survey. https://doi.org/10.5066/F7G15Z17.

Houser, C., P. Wernette, E. Rentschlar, H. Jones, B. Hammon, and S. Trimble. 2015. Post-storm beach and dune recovery: implications for barrier island resilience. *Geomorphology* 234: 54–63. https://doi.org/10.1016/j.geomorph.2014.12044.

Jensen, F.V., and T.D. Nielsen. 2007. *Bayesian networks and decision graphs*. New York: Springer. https://doi.org/10.1007/978-0-387-68282-2.

Kratzmann, M.G., and C.J. Hapke. 2012. Quantifying anthropogenically driven morphologic changes on a barrier island: Fire Island National Seashore, New York. *Journal of Coastal Research* 28 (1): 76–88. https://doi.org/10.2112/JCOASTRES-D-10-00012.1.

Leatherman, S.P. 1985. Geomorphic and stratigraphic analysis of Fire Island, New York. *Marine Geology* 63 (1-4): 173–195.

Lee, G., R.J. Nicholls, and W.A. Birkemeier. 1998. Storm-driven variability of the beach-nearshore profile at duck, North Carolina, USA, 1981-1991. *Marine Geology* 148 (3-4): 163–177.

Lentz, E.E., and C.J. Hapke. 2011. Geologic framework influences on the geomorphology of an anthropogenically modified barrier island: assessment of dune/beach changes at Fire Island, New York. *Geomorphology* 126 (1-2): 82–96. https://doi.org/10.1016/j.geomorph.2010.10.032.

Lentz, E.E., C.J. Hapke, H.F. Stockdon, and R.E. Hehre. 2013. Improving understanding of near-term barrier island evolution through multi-decadal assessment of morphologic change. *Marine Geology* 337: 125–139. https://doi.org/10.1016/j.margeo.2013.02.004.

Lentz, E.E., E.R. Thieler, N.G. Plant, S.R. Stippa, R.M. Horton, and D.B. Gesch. 2016. Evaluation of dynamic coastal response to sea-level rise modifies inundation likelihood. *Nature Climate Change* 6 (7): 696–700. https://doi.org/10.1038/NCLIMATE2957.

Long, J.W., N.G. Plant, P.S. Dalyander, and D.M. Thompson. 2014. Probabilistic method for constructing wave time series at inshore locations using model scenarios. *Coastal Engineering* 89: 53–62. https://doi.org/10.1016/j.coastaleng.2014.03.008.

Lorenzo-Trueba, J., and A.D. Ashton. 2014. Rollover, drowning, and discontinuous retreat: distinct modes of barrier response to sea-level rise arising from a simple morphodynamic model. *Journal of Geophysical Research: Earth Surface* 119 (4): 779–801. https://doi.org/10.1002/2013JF002941.

Melillo JM, Richmond TC, Yohe GW, Eds. 2014. Climate change impacts in the United States: the third national climate assessment. U.S. Global Change Research Program, 841 pp. https://doi.org/10.7930/J0Z31WJ2.

Miller, J.K., and R.G. Dean. 2004. A simple new shoreline change model. *Coastal Engineering* 51 (7): 531–556. https://doi.org/10.1016/j.coastaleng.2004.05.006.

Morton, R.A., and A.H. Sallenger. 2003. Morphologic impacts of extreme storms on sandy beaches and barriers. *Journal of Coastal Research* 19 (3): 560–573.

Morton, R.A., J.G. Paine, and J.C. Gibeaut. 1994. Stages and durations of post storm beach recovery, southeastern Texas coast, U.S.a. *Journal of Coastal Research* 10 (4): 884–908.

Norsys Software Corp. 2010. Netica-J Manual Version 4.18. Vancouver, Canada.

Palmsten, M.L., K.T. Holland, and N.G. Plant. 2013. Velocity estimation using a Bayesian network in a critical-habitat reach of the Kootenai River, Idaho. *Water Resources Research* 49 (9): 5865–5879. https://doi.org/10.1002/wrcr.20361.

Palmsten, M.L., K.D. Splinter, N.G. Plant, and H.F. Stockdon. 2014. Probabilistic estimation of dune retreat on the Gold Coast, Australia. *Shore and Beach* 4: 35–43.

Pelnard-Considere, R. 1956. Essai de theorie do l'evolution des forms de rivageen plage de sable et de galets, *4me Journees de l'Hydraulique, Les Energies de la Mer*, Question III, Rapport No. 1: 289–298, Societe Hydrotechnique de France, Paris, France.

Plant, N.G., and K.T. Holland. 2011. Prediction and assimilation of surf-zone processes using a Bayesian network part I: forward models. *Coastal Engineering* 58 (1): 119–130. https://doi.org/10.1016/j.coastaleng.2010.09.003.

Plant, N.G., and H.F. Stockdon. 2012. Probabilistic prediction of barrier-island response to hurricanes. *Journal of Geophysical Research* 117 (F3): F03015. https://doi.org/10.1029/2011JF002326.

Plant, N.G., J. Flocks, H.F. Stockdon, J.W. Long, K. Guy, D.M. Thompson, J.M. Cormier, C.G. Smith, J.L. Miselis, and P.S. Dalyander. 2014. Predictions of barrier island berm evolution in time-varying storm climatology. *Journal of Geophysical Research: Earth Surface* 119 (2): 300–316. https://doi.org/10.1002/2013JF002871.

Plant, N.G., E.R. Thieler, and D.L. Passeri. 2016. Coupling centennial-scale shoreline change to sea-level rise and coastal morphology in the Gulf of Mexico using a Bayesian network. *Earth's Future* 4 (5): 143–157. https://doi.org/10.1002/2015EF000331.

Priestas, A.M., and S. Fagherazzi. 2010. Morphological barrier island changes and recovery of dunes after hurricane Dennis, St. George Island, Florida. *Geomorphology* 114 (3-4): 614–626. https://doi.org/10.1016/j.geomorph.2009.09.002.

Program for the study of developed shorelines, 2017. https://psds.wcu.edu/. [13 June 2017].

Reeve, D.E., H. Karunarathna, S. Pan, J.M. Horrillo-Caraballo, G. Rozynski, and R. Ranasinghe. 2016. Data-driven and hybrid coastal morphological prediction methods for mesoscale forecasting. *Geomorphology* 256: 49–67. https://doi.org/10.1016/j.geomorph.2015.10.016.

Riggs, S.R., W.J. Cleary, and S.W. Snyder. 1995. Influence of inherited geologic framework on barrier shoreface morphology and dynamics. *Marine Geology* 126 (1-4): 213–234.

Roelvink, D., A. Reniers, A. van Dongeren, J. van Thiel de Vries, R. McCall, and J. Lescinski. 2009. Modelling storm impacts on beaches, dunes and barrier islands. *Coastal Engineering* 56 (11–12): 1133–1152. https://doi.org/10.1016/j.coastaleng.2009.08.006.

Safak, I., J.C. Warner, and J.H. List. 2016. Barrier island breach evolution: alongshore transport and bay-ocean pressure gradient interactions. *Journal of Geophysical Research Oceans* 121 (12): 8720–8730. https://doi.org/10.1002/2016JC012029.

Safak, I., J.H. List, J.C. Warner, and W.C. Schwab. 2017. Persistent shoreline shape induced from offshore geologic framework: effects of shoreface connected ridges. *Journal of Geophysical Research: Oceans* 122 (11): 8721–8738. https://doi.org/10.1002/2017JC012808.

Schwab, W.C., E.R. Thieler, J.R. Allen, D.S. Foster, B.A. Swift, and J.F. Denny. 2000. Influence of inner-continental shelf geologic framework on the evolution and behavior of the barrier-island system between Fire Island inlet and Shinnecock inlet, Long Island, New York. *Journal of Coastal Research* 16: 408–422.

Schwab, W.C., W.E. Baldwin, C.J. Hapke, E.E. Lentz, P.T. Gayes, J.F. Denny, P.T. Gayes, and J.C. Warner. 2013. Geologic evidence for onshore sediment transport from the inner-continental shelf: Fire Island, New York. *Journal of Coastal Research* 29 (3): 536–544.

Schwab, W.C., W.E. Baldwin, J.F. Denny, C.J. Hapke, P.T. Gayes, J.H. List, and J.C. Warner. 2014. Modification of the quaternary stratigraphic framework of the inner-continental shelf by Holocene marine transgression: an example offshore of Fire Island, New York. *Marine Geology* 355: 346–360. https://doi.org/10.1016/j.margeo.2014.06.011.

Short, A.D., and P.A. Hesp. 1982. Wave, beach and dune interactions in southeastern Australia. *Marine Geology* 48 (3-4): 259–284.

Splinter, K.D., I.L. Turner, M.A. Davidson, P. Barnard, B. Castelle, and J. Oltman-Shay. 2014. A generalized equilibrium model for predicting daily to interannual shoreline response. *Journal of Geophysical Research: Earth Surface* 119 (9): 1936–1958. https://doi.org/10.1002/2014JF003106.

Splinter, K.D., I.L. Turner, M. Reinhardt, and G. Ruessink. 2017. Rapid adjustment of shoreline behavior to changing seasonality of storms: observations and modelling at an open-coast beach. *Earth Surface Processes and Landforms* 42 (8): 1186–1194. https://doi.org/10.1002/esp.4088.

Stockdon, H.F., R.A. Holman, P.A. Howd, and A.H. Sallenger. 2006. Empirical parameterization of setup, swash, and runup. *Coastal Engineering* 53 (7): 573–588. https://doi.org/10.1016/j.coastaleng.2005.12.005.

Stockdon, H.F., A.H. Sallenger Jr., R.A. Holman, and P.A. Howd. 2007. A simple model for the spatially-variable coastal response to hurricanes. *Marine Geology* 238 (14): 1–20. https://doi.org/10.1016/j.margeo.2006.11.004.

Turner, I.L., M.D. Harley, A.D. Short, J.A. Simmons, M.A. Bracs, M.S. Phillips, and K.D. Splinter. 2016. A multi-decade dataset of monthly beach profile surveys and inshore wave forcing at Narrabeen.

Australia. Scientific Data 3: 160024. https://doi.org/10.1038/sdata.2016.24.

U.S. Climate Change Science Program. 2009. Coastal sensitivity to sea-level rise: A Focus on the Mid-Atlantic Region. A report by the U.S. Climate Change Science Program and the Subcommittee on Global Change Research. U.S. Environmental Protection Agency, Washington D.C., USA, 320 pp.

Warner, J.C., J.H. List, W.C. Schwab, G. Voulgaris, B.N. Armstrong, and N. Marshall. 2014. Inner-shelf circulation and sediment dynamics on a series of shoreface connected ridges offshore of Fire Island, New York. *Ocean Dynamics* 64 (2): 1767–1781.

Warner, J.C., W.C. Schwab, J.H. List, I. Safak, M. Liste, and W. Baldwin. 2017. Inner-shelf ocean dynamics and seafloor morphologic changes during Hurricane Sandy. *Continental Shelf Research* 138: 1–8. https://doi.org/10.1016/j.csr.2017.02.003.

Wilson, K.E., P.N. Adams, C.J. Hapke, E.E. Lentz, and O.T. Brenner. 2015. Application of Bayesian networks to hindcast barrier island morphodynamics. *Coastal Engineering* 102: 30–43. https://doi.org/10.1016/j.coastaleng.2015.04.006.

Wilson, K.E., C.J. Hapke, R.E. Henderson, E.E. Lentz, J.L. Miselis, and P.M. Weppler. 2017. *Post-hurricane Sandy Beach profile survey—Fire Island inlet to Moriches inlet 2013*. Reston, VA: U.S. Geological Survey Data Release. U.S. Geological Survey. https://doi.org/10.5066/F7XK8CSR.

Wright LD, Short AD. 1984. Morphodynamic variability of surf zones and beaches: a synthesis. *Marine Geology* 56: 93–118.

Wright, L.D., A.D. Short, and M. Green. 1985. Short-term changes in the morphodynamic states of beaches and surf zones: an empirical predictive model. *Marine Geology* 62 (3–4): 339–364.

Yang, S.L., J. Zhang, J. Zhu, P. Smith, S.B. Dai, A. Gao, and P. Li. 2005. Impacts of dams on Yangtze River sediment supply to the sea and delta intertidal wetland response. *Journal of Geophysical Research: Earth Surface* 110 (F3): F03006. https://doi.org/10.1029/2004JF000271.

Yates, M.L., R.T. Guza, and W.C. O'Reilly. 2009. Equilibrium shoreline response: observations and modeling. *Journal of Geophysical Research* 114 (C9): C09014. https://doi.org/10.1029/2009JC005359.